Contribution from the Laboratoire de Chimie Théorique,§ Université de Paris-Sud, 91405 Orsay, France, and Department of Chemistry, North Carolina State University, Raleigh, North Carolina 27695-8204

Semimetallic versus Semiconducting Properties of MX_2 Layer Compounds Containing d^2 Metal Ions

Enric Canadell*,† and Myung-Hwan Whangbo*,‡

Received August 4, 1989

Electronic structures of $CrNb_2Se_4$, β-$MoTe_2$, and α-ZrI_2 were examined by performing tight-binding band calculations. Our study suggests that the electronic properties of $M'Nb_2Se_4$ (M' = Ti, V, Cr) are more consistent with the oxidation state of +2 for M' rather than that of +3. α-ZrI_2 and β-$MoTe_2$ are semiconducting and semimetallic, respectively, despite their structural similarity and identical d-electron count on the metal (i.e., d^2). The structural origin of this difference was also examined.

Many layered compounds contain MX_2 layers made up of MX_6 octahedra.[1] In MX_2 layers containing d^2 metal ions, metal atoms are found to cluster to form zigzag chains.[2-5] It is convenient to regard such an MX_2 layer as made up of M_2X_6 double octahedral chains (**1**) having zigzag metal-metal bonds (i.e., dashed

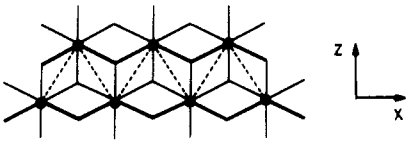

1

lines in **1**),[6] since the electronic structure of the MX_2 layer closely resembles that of its constituent M_2X_6 chain.[6] For the M_2X_6 chain **1** with X = S or Se, the bottom four of its six t_{2g}-block bands overlap[6,7] and hence become partially filled for d^2 metal ions, so that MX_2 layers with d^2 metal ions are expected to be metals. The present work is concerned with d^2 metal ions, i.e., $M'Nb_2Se_4$ (M' = Ti, V, Cr),[3] β-$MoTe_2$,[4] and α-ZrI_2.[5] Both $M'Nb_2Se_4$[3a] and β-$MoTe_2$[4e] are metals, as expected, but they exhibit resistivity anomalies at low temperature.[3a,4c,d] α-ZrI_2 is a semiconductor with activation energy of 0.1 eV,[5] although it is quite similar in structure to the MX_2 layers of $M'Nb_2Se_4$ and β-$MoTe_2$. We examine the electronic properties of these systems by performing tight-binding band electronic structure calculations[8] on the basis of the extended Hückel method.[9] The atomic parameters employed in our study are summarized in Table I.

Crystal Structure

A perspective view of the M_2X_6 double octahedral chain **1** is shown in **2**, where each MX_6 octahedron represents a single octahedral chain of **1**. The projection view of **2** along the chain is

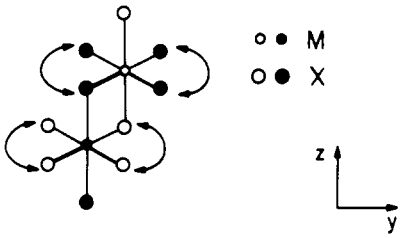

2

given by **3**, where two chalcogen atoms indicated by a double-

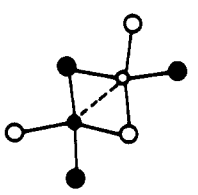

3

Table I. Parameters and Exponents Used in the Calculations

atom	orbital	H_{ii}, eV	ζ_1	ζ_2	c_1[a]	c_2[a]
Se[12]	4s	-20.50	2.44			
	4p	-13.20	2.07			
Te[13]	5s	-20.78	2.51			
	5p	-13.20	2.16			
I[14]	5s	-18.00	2.679			
	5p	-12.70	2.322			
Nb[15]	5s	-10.10	1.90			
	5p	-6.86	1.85			
	4d	-12.10	4.08	1.64	0.6401	0.5516
Mo[15]	5s	-8.34	1.96			
	5p	-5.24	1.90			
	4d	-10.50	4.54	1.90	0.5899	0.5899
Zr[12]	5s	-8.00	1.817			
	5p	-5.40	1.776			
	4d	-10.20	3.835	1.505	0.6210	0.5796

[a] Contraction coefficients used in the double-ζ expansion.

headed arrow are projected as one chalcogen atom. According to this projection view, an MX_2 layer with d^2 metal ions is represented by **4**.[6] It is such MX_2 layers that stack to form

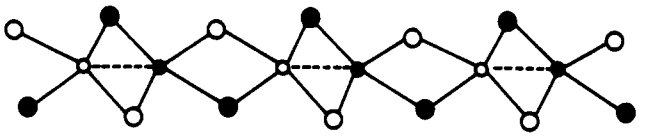

4

three-dimensional lattices in $M'Nb_2Se_4$ (M' = Ti, V, Cr), β-$MoTe_2$, and α-ZrI_2. In $M'Nb_2Se_4$, the M' atoms occupy half the octahedral sites between $NbSe_2$ layers.

Band Electronic Structures

A. $M'Nb_2Se_4$ (M' = Ti, V, Cr). In understanding the electrical properties of $M'Nb_2Se_4$, it is crucial to know the oxidation state

† Université de Paris-Sud.
‡ North Carolina State University.
§ The Laboratoire de Chimie Théorique is associated with the CNRS (UA 506) and is a member of the ICMO and the IPCM (Orsay, France).

(1) Hulliger, F. In *Structural Chemistry of Layer-Type Phases*; Lévy, F., Ed.; Reidel: Dordrecht, The Netherlands, 1976.
(2) Kadijk, F.; Huisman, R.; Jellinek, F. *Acta Crystallogr.* **1968**, *B24*, 1102.
(3) (a) Meerschaut, A.; Spiesser, M.; Rouxel, J.; Gorochov, O. *J. Solid State Chem.* **1980**, *31*, 31. (b) Meerschaut, A.; Rouxel, J. *C. R. Seances Acad. Sci., Ser. C* **1977**, *277*, 163.
(4) (a) Brown, B. E. *Acta Crystallogr.* **1986**, *20*, 268. (b) Manolikas, C.; van Landuyt, J.; Amelinckx, S. *Phys. Status Solidi A* **1979**, *53*, 327. (c) Hughes, H. P.; Friend, R. H. *J. Phys. C* **1978**, *11*, L103. (d) Clarke, R.; Marseglia, E.; Hughes, H. P. *Philos. Mag. B* **1978**, *38*, 121. (e) Wilson, J. A.; Yoffe, A. D. *Adv. Phys.* **1969**, *18*, 193. (f) Vellinga, M. B.; de Jonge, R.; Haas, C. *J. Solid State Chem.* **1970**, *2*, 299.
(5) Guthrie, D. H.; Corbett, J. D. *J. Solid State Chem.* **1981**, *37*, 256.
(6) Canadell, E.; Le Beuze, A.; El Khalifa, M. A.; Chevrel, R.; Whangbo, M.-H. *J. Am. Chem. Soc.* **1989**, *111*, 3778.
(7) Canadell, E.; Whangbo, M.-H. *Inorg. Chem.* **1986**, *25*, 1488.
(8) Whangbo, M.-H.; Hoffmann, R. *J. Am. Chem. Soc.* **1978**, *100*, 6093.
(9) Hoffmann, R. *J. Chem. Phys.* **1963**, *39*, 1397. A modified Wolfsberg-Helmholz formula was used to calculate the off-diagonal H_{ij} values: Ammeter, J. H.; Bürgi, H.-B.; Thibeault, J.; Hoffmann, R. *J. Am. Chem. Soc.* **1978**, *100*, 3686.

0020-1669/90/1329-1398$02.50/0

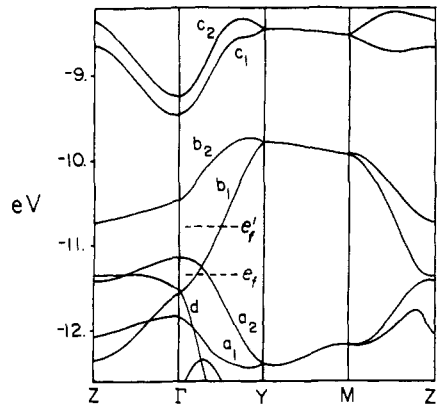

Figure 1. Dispersion relations of the t_{2g}-block bands (a, b, and c) of a single $NbSe_2$ layer, where $\Gamma = (0, 0)$, $Y = (b^*/2, 0)$, $M = (b^*/2, c^*/2)$, and $Z = (0, c^*/2)$. The Fermi levels e_f and e_f' refer to the d^2 and $d^{2.5}$ electron countings, respectively. The $\Gamma \rightarrow Y$ and $\Gamma \rightarrow Z$ directions refer to the intra- and the interchain directions, respectively.

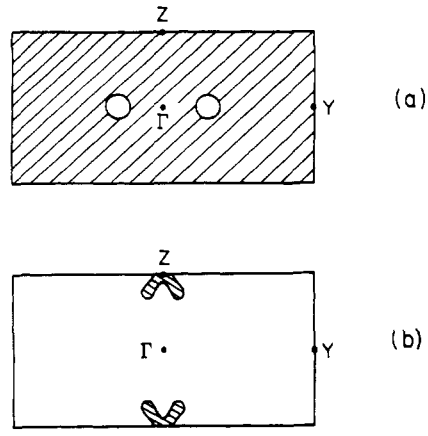

Figure 2. Hole (a) and electron Fermi surfaces (b) associated with the d^2 electron counting (e_f) of Figure 1. The shaded and unshaded regions of wave vector lead to filled and unfilled band levels respectively.

of M′. The $NbSe_2$ layers have zigzag metal chains as in β-$MoTe_2$ and α-ZrI_2, so that the electron count on Nb is expected to be d^2. This requires the oxidation state of 2+ for M′, which seems consistent with the magnetic properties of $M'Nb_2Se_4$: For example, the effective magnetic moment of Cr in $CrNb_2Se_4$ is 4.4 μ_B,[3a] which is quite close to that of Cr^{2+} found for $CrMo_2S_4$ (i.e., 4.6 ± 0.1 μ_B).[10] Figure 1 shows the dispersion relations calculated for the t_{2g}-block bands (a, b, and c) of a single $NbSe_2$ layer taken from the crystal structure of $CrNb_2Se_4$.[3a] As described elsewhere,[7] bands a and c result from the metal–metal bonding and antibonding levels of zigzag metal–metal bonds, respectively, while band b originates from the metal $x^2 - y^2$ orbitals. The latter describe 1,3-interactions in each zigzag metal chain. Band d overlapping the bottom portion of the t_{2g}-block bands is the top of the Se p-block bands. The Fermi level e_f of Figure 1 corresponds to the d^2 electron counting. The partially filled bands of Figure 1 lead to a hole and an electron Fermi surface shown in parts a and b of Figure 2, respectively, which show that the $NbSe_2$ layer is a semimetal. This conclusion is consistent with the results of the Hall coefficient measurements on $M'Nb_2Se_4$.[3a] The hole pockets of Figure 2 are nested by the vector $q \cong 0.29b^*$. Thus, an electronic instability associated with this nesting might be

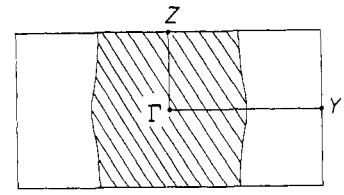

Figure 3. Fermi surface associated with the $d^{2.5}$ electron counting (e_f) of Figure 1. The shaded and unshaded regions of wave vectors lead to filled and unfilled band levels, respectively.

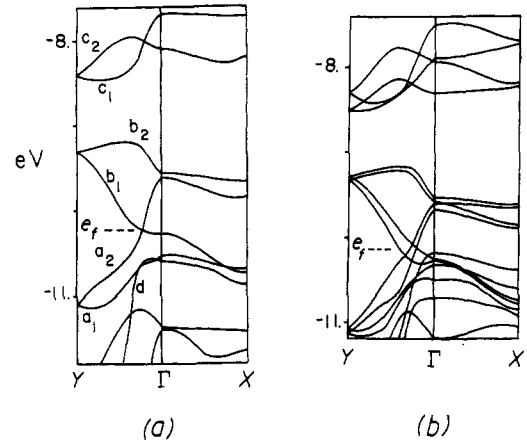

Figure 4. Dispersion relations of the t_{2g}-block bands calculated for (a) a single $MoTe_2$ layer and (b) the 3D β-$MoTe_2$ lattice. $\Gamma = (0, 0)$, $X = (a^*/2, 0)$ and $Y = (0, b^*/2)$ for the $MoTe_2$ layer, and $\Gamma = (0, 0, 0)$, $X = (a^*/2, 0, 0)$ and $Y = (0, b^*/2, 0)$ for the 3D β-$MoTe_2$ lattice. The $\Gamma \rightarrow X$ and $\Gamma \rightarrow Y$ directions represent the inter- and the intrachain directions, respectively. The dashed line refers to the Fermi level.

responsible for a weak resistivity upturn of $CrNb_2Se_4$ at ~50 K.[3a] However, such a resistivity upturn is absent in $TiNb_2Se_4$ and VNb_2Se_4.[3a] An electronic factor responsible for this observation might be that the hole pockets of $TiNb_2Se_4$ and VNb_2Se_4 are not large enough.

The above discussion is based upon the assumption of d^2 electron counting for Nb. If the M′ atoms of $M'Nb_2Se_4$ have the oxidation state +3, as suggested by Meerschaut et al.,[3a] the electron count on Nb becomes $d^{2.5}$. This raises the Fermi level to e_f' in Figure 1, thereby making band b_1 half-filled. Consequently, the resulting Fermi surface, shown in Figure 3, is one-dimensional in nature, and is nested by a vector $q = 0.5b^* + 0.5c^*$. One may rationalize the resistivity upturn of $CrNb_2Se_4$, which occurs at 50 K,[3a] as a consequence of an electronic instability associated with this nesting. According to this reasoning, $TiNb_2Se_4$ and VNb_2Se_4 are expected to exhibit a similar resistivity anomaly as in $CrNb_2Se_4$, in disagreement with experiment.[3a] Slight differences in the Nb_2Se_4 layer structures of $M'Nb_2Se_4$ induced by the different M′ atoms would have stronger effects on their electronic properties when their Fermi surfaces are given by Figure 2 rather than by Figure 3. Thus, the available resistivity data on $TiNb_2Se_4$ and VNb_2Se_4 are more consistent with the semimetallic band picture based upon a d^2 electron counting on Nb.

B. β-$MoTe_2$. Due to displacive movement between $MoTe_2$ layers, β-$MoTe_2$ shows a resistivity anomaly at about 250 K.[4b-e] This suggests that the nature of the partially filled bands of β-$MoTe_2$ is affected by a slight change in $MoTe_2$ layers. Figure 4a shows the dispersion relations calculated for the t_{2g}-block bands of a single $MoTe_2$ layer. In general, the t_{2g}-block bands, a, b, and c of the $MoTe_2$ layer are similar to the corresponding ones of the $NbSe_2$ layer (Figure 1). At Γ, the top of band a_2 is close in energy to the bottom of band b_2 in the $MoTe_2$ layer while this is not the case in the $NbSe_2$ layer. This is caused by the fact that the top of the Te p-block bands lies considerably higher in energy than that of the Se p-block bands. Along $\Gamma \rightarrow Y$ of Figure 4a, bands a_2 and d have the same symmetry so that they mix. Band a_2 has more metal d-orbital character near Y but more Te p-orbital character near Γ.

(10) Chevrel, R.; Sergent, M.; Meury, J. L.; Quan, D. T.; Colin, Y. *J. Solid State Chem.* **1974**, *10*, 260.
(11) (a) Alcock, N. W.; Kjekshus, A. *Acta Chem. Scand.* **1965**, *19*, 79. (b) Wildervanck, J. C.; Jellinek, F. *J. Less-Common Met.* **1971**, *24*, 73.
(12) Canadell, E.; Whangbo, M.-H. *Inorg. Chem.* **1987**, *26*, 3974.
(13) Canadell, E.; Mathey, Y.; Whangbo, M.-H. *J. Am. Chem. Soc.* **1988**, *110*, 104.
(14) Whangbo, M.-H.; Foshee, M. J. *Inorg. Chem.* **1981**, *20*, 113.
(15) Summerville, R. H.; Hoffmann, R. *J. Am. Chem. Soc.* **1976**, *98*, 7240.

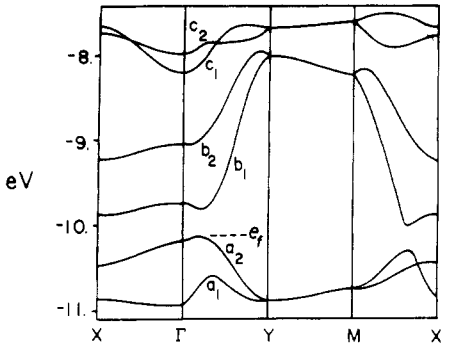

Figure 5. Dispersion relations of the t_{2g}-block bands calculated for a single ZrI_2 layer, where $\Gamma = (0, 0)$, $X = (a^*/2, 0)$, $M = (a^*/2, b^*/2)$ and $Y = (0, b^*/2)$. The $\Gamma \rightarrow X$ and $\Gamma \rightarrow Y$ directions represent the inter- and the intrachain directions, respectively. The dashed line refers to the Fermi level.

Figure 4b shows the t_{2g}-block bands calculated for the three-dimensional (3D) β-$MoTe_2$ lattice. With respect to the case of a single $MoTe_2$ layer, all the band levels are doubled in β-$MoTe_2$ since it has two $MoTe_2$ layers per unit cell. Figure 4b shows that this band doubling does not lead to nearly degenerate bands but to substantially split ones. Namely, the t_{2g}-block bands of β-$MoTe_2$ reflect appreciable interlayer Te···Te interactions. This is possible since the t_{2g}-block bands have large Te p-orbital character and since $MoTe_2$ layers interact via short Te···Te contacts (e.g., 3.86 and 3.91 Å) smaller than the van der Waals radii sum of 4.20 Å. With d^2 metal ions, the Fermi level cuts the bands arising from the t_{2g}-block bands a_2 and b_1. It is clear from Figure 4b that this will lead to hole and electron Fermi surfaces, and hence β-$MoTe_2$ is a semimetal. Since a displacive movement of $MoTe_2$ layers will modify the interlayer Te···Te contact distances, the band splittings of Figure 4b will also change so that the resulting hole and electron Fermi surfaces will be slightly different. Consequently, the electrical resistivity of β-$MoTe_2$ should be affected by a displacive movement of $MoTe_2$ layers.

C. α-ZrI_2. Figure 5 shows the t_{2g}-block bands of a single ZrI_2 layer. In contrast to the case of $NbSe_2$ and $MoTe_2$ layers, the bottom two of the t_{2g}-block bands are separated from the rest, thereby leading to a band gap. The top of the iodine p-block bands lies below the t_{2g}-block bands, and hence are not shown in Figure 5. As in β-$MoTe_2$, α-ZrI_2 has two ZrI_2 layers per unit cell.[5] Our band calculations on the 3D α-ZrI_2 lattice show that each band of Figure 5 splits into two, thereby reducing the band gap. It is clear from Figures 1, 4a, and 5 that the presence of a band gap in α-ZrI_2 is caused by the fact that band a_2 lies below band b_1. We now examine why this happens for α-ZrI_2 but not for $M'Nb_2Se_4$ and β-$MoTe_2$. Shown in **5**–**7** are various bond angles

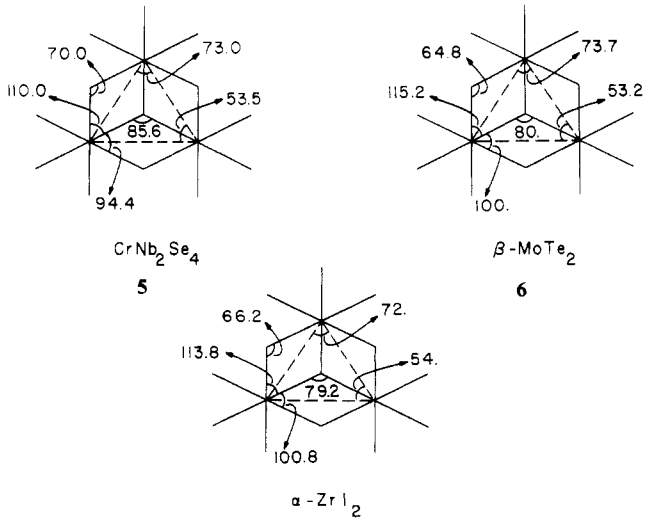

$CrNb_2Se_4$ **5** β-$MoTe_2$ **6**

α-ZrI_2 **7**

associated with three adjacent MX_6 octahedra found in the $NbSe_2$, $MoTe_2$ and ZrI_2 layers, respectively. Clearly, the MX_6 octahedra of $M'Nb_2Se_4$, β-$MoTe_2$, and α-ZrI_2 are remarkably similar in shape. This distortion of MX_6 octahedra could not have induced the difference in their electronic structures.

The electronegativity difference between M and X can affect the extent of orbital mixing between the two atoms. To examine how strongly our results are influenced by this factor, we calculated the band structure of the $NbSe_2$ layer using the H_{ii} (valence shell ionization potential) values of Zr and I and that of the ZrI_2 layer using the H_{ii} values of Nb and Se. These calculations still show that bands a_2 and b_1 are overlapping in the $NbSe_2$, but are separated in the ZrI_2 layer. Thus the difference in the H_{ii} values of M and X is not responsible for why the electronic structure α-ZrI_2 differs from that of $M'Nb_2Se_4$ or β-$MoTe_2$.

It is noted that Figures 1, 4a, and 5 that, along the chain direction, bands a_2 and b_1 have different symmetries and hence overlap when band a_2 is raised high enough in energy, thereby leading to a metallic situation for d^2 metal systems. Bands a_2 and d have the same symmetry, so that band a_2 lies high in energy when the p-block band of X lies high in energy. To have bands a_2 and b_1 overlapping, therefore, the p-block band of X should be high in energy. The latter requires strong antibonding in intralayer X···X contacts. The relevant X···X distances in the $NbSe_2$, $MoTe_2$, and ZrI_2 layers are summarized in **8**–**10**, respectively. Clearly, the X···X contact distances are much longer in the ZrI_2 layer than in the $NbSe_2$ or $MoTe_2$ layer, which is a direct consequence of the fact that the Zr–I bonds are much longer than the Nb–Se and Mo–Te bonds. In addition, iodine has more contracted orbitals than does tellurium. Consequently, the top of the iodine p-block bands lies considerably lower in energy compared with that of the tellurium or selenium p-block bands. This explains why bands a_2 and b_1 overlap in the $NbSe_2$ and $MoTe_2$ layers but not in the ZrI_2 layer.

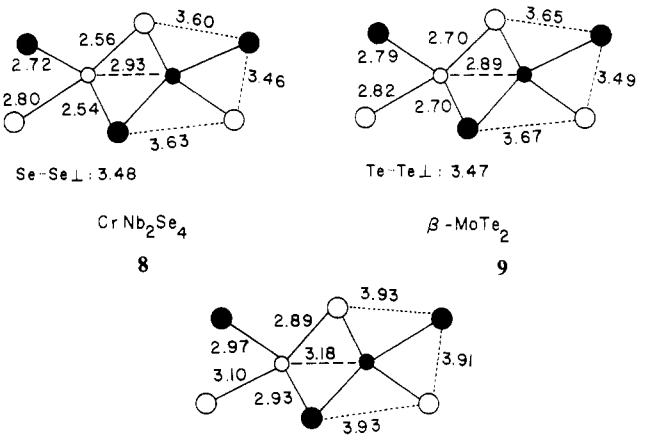

$CrNb_2Se_4$ **8** β-$MoTe_2$ **9**

α-ZrI_2 **10**

Concluding Remarks

β-$MoTe_2$ and α-ZrI_2 are structurally similar in that they all contain MX_2 layers of d^2 metal ions. Nevertheless, β-$MoTe_2$ is a semimetal while α-ZrI_2 is a semiconductor. This difference originates from the fact that, in contrast to the case of β-$MoTe_2$, the top of the p-block bands of X lies below the bottom of the metal t_{2g}-block bands in α-ZrI_2 due to the long intralayer I···I contact distances. Our calculations on β-$MoTe_2$ show that the partially filled t_{2g}-block bands of β-$MoTe_2$ contain a sizable contribution from tellurium p-orbitals, so the hole and electron Fermi surfaces resulting from them are expected to be affected by a slight change in the interlayer Te···Te contact distances.

$M'Nb_2Se_4$ (M' = Ti, V, Cr) phases are structurally similar to β-$MoTe_2$ and α-ZrI_2. Our calculations show that if the oxidation state of M' is +2 $M'Nb_2Se_4$ phases are two-dimensional semi-

metals with small hole and electron pockets. If the oxidation state of M′ is +3, $M'Nb_2Se_4$ phases are calculated to be one-dimensional metals. Therefore, it would be interesting to measure the resistivity anisotropy as well as the possible superlattice modulation of these compounds.

Acknowledgment. This work was supported by NATO, Scientific Affairs Division, and also by DOE, Office of Basic Sciences, Division of Materials Science, under Grant DE-FG05-86ER45259. We are thankful to Dr. A. Meerschaut for references and valuable comments.

Contribution from the Laboratoire de Chimie Théorique (CNRS URA 506) and Laboratoire de Physique des Solides (CNRS LA 2), Université de Paris-Sud, 91405 Orsay, France, Laboratoire de Chimie des Solides, IPCM, Université de Nantes, 44072 Nantes, France, and Department of Chemistry, North Carolina State University, Raleigh, North Carolina 27695-8204

Comparison of the Electronic Structures of Layered Transition-Metal Trichalcogenides $TaSe_3$, TaS_3, and $NbSe_3$

E. Canadell,*,† I. E.-I. Rachidi,† J. P. Pouget,*,‡ P. Gressier,§ A. Meerschaut,§ J. Rouxel,*,§ D. Jung,∥ M. Evain,∥ and M.-H. Whangbo*,∥

Received August 22, 1989

The electronic structures of the three layered transition-metal trichalcogenides $NbSe_3$, TaS_3, and $TaSe_3$ were examined by performing tight-binding band electronic structure calculations. The Fermi surfaces of these materials were also calculated to analyze their metallic and/or charge density wave properties. In these trichalcogenides MX_3 (M = Nb, Ta; X = S, Se) made up of prismatic MX_3 chains, the broken X-X bonds of their equilateral-like MX_3 chains and the short intra- and interlayer X···X contacts are found to be crucial for the semimetallic properties of $TaSe_3$ and for the charge density wave phenomena of $NbSe_3$ and TaS_3. For the electronic parameters of the charge density waves in $NbSe_3$ and TaS_3, a quantitative agreement is obtained between the experimental observations and the present band electronic structure calculations.

Layered transition-metal trichalcogenides MX_3 (M = Nb, Ta; X = S, Se) contain layers made up of trigonal-prismatic chains.[1] These MX_3 prismatic chains are classified as isosceles- or equilateral-like depending upon whether the oxidation state of the X_3 triangle forming the base of the MX_6 prism is $(X^{2-} + X_2^{2-})$ or $3X^{2-}$, respectively.[2] For simplicity, isosceles- and equilateral-like prismatic chains may be referred to as I- and E-prismatic chains, respectively. Thus $NbSe_3$ and monoclinic TaS_3 each have four I- and two E-prismatic MX_3 chains per unit cell, while $TaSe_3$ has two I- and two E-prismatic chains per unit cell. Consequently, it is expected that $NbSe_3$ and TaS_3 each have two d electrons per unit cell but $TaSe_3$ has none. In agreement with this simple electron counting, both $NbSe_3$ and TaS_3 are metals at room temperature. When the temperature is lowered, both undergo two different charge density wave (CDW) transitions. At the end of these two transitions, TaS_3 becomes a semiconductor but $NbSe_3$ remains metallic.[1] The above electron counting on $TaSe_3$ suggests that $TaSe_3$ would be a semiconductor, but it is a semimetal[1]. Although a number of band electronic structure studies on $NbSe_3$[3] and $TaSe_3$[4] have been reported, there has been no systematic study concerning how $NbSe_3$ and TaS_3 differ in their electronic structures and why $TaSe_3$ is semimetallic from the viewpoint of their crystal structures. In addition, Fermi surfaces have not been reported for TaS_3 and $TaSe_3$. Therefore, we carry out tight-binding band electronic structure calculations[5] on $NbSe_3$, TaS_3, and $TaSe_3$ within the framework of the extended Hückel method[6] and discuss similarities and differences in their electronic structures. The atomic parameters employed in our study are summarized in Table I.

Table I. Exponents and Parameters Used in the Calculations

atom	orbital	H_{ii}, eV	ζ_1	ζ_2	c_1[a]	c_2[a]
Nb	5s	-10.10	1.90			
	5p	-6.86	1.85			
	4d	-12.10	4.08	1.64	0.6401	0.5516
Ta	6s	-10.10	2.28			
	6p	-6.86	2.24			
	5d	-12.10	4.76	1.94	0.6597	0.5589
S	3s	-20.00	1.817			
	3p	-13.30	1.817			
Se	4s	-20.50	2.44			
	4p	-13.20	2.07			

[a] Contraction coefficients used in the double-ζ expansion.

Table II. Short X-X and X···X Distances (Å) in $NbSe_3$, TaS_3, and $TaSe_3$ Shown in **1** and **2**

dist	$NbSe_3$	TaS_3	$TaSe_3$
A	2.37	2.07	2.58
A′	2.50	2.11	
B	2.73	2.80	2.66
C	2.92	2.84	2.90
D	3.30	3.26	3.49
E	2.92	2.92	

Crystal Structures and Short X···X Contacts

In the layered trichalcogenide $ZrTe_3$, composed exclusively of I-prismatic chains, short intra- and interlayer Te···Te are found to play a crucial role for its semimetallic property and resistivity anomaly.[7] By analogy, one might expect short X···X contacts of MX_3 (M = Nb, Ta; X = S, Se) to be also important in determining the electronic properties of MX_3. The projection view along the chain direction (i.e., the *b*-axis direction) of $NbSe_3$[8] and

† Laboratoire de Chimie Théorique, Université de Paris-Sud.
‡ Laboratoire de Physique des Solides, Université de Paris-Sud.
§ Université de Nantes.
∥ North Carolina State University.

(1) Reviews: (a) Meerschaut, A.; Rouxel, J. In *Crystal Chemistry and Properties of Materials with Quasi-One-Dimensional Structures*; Rouxel, J., Ed.; Reidel: Dordrecht, The Netherlands, 1986; p 205. (b) Monceau, P. In *Electronic Properties of Inorganic Quasi-One-Dimensional Compounds*; Monceau, P., Ed.; Reidel: Dordrecht, The Netherlands, 1985; Part II, p 139.
(2) Whangbo, M.-H. In *Crystal Chemistry and Properties of Materials with Quasi-One-Dimensional Structures*; Rouxel, J., Ed.; Reidel: Dordrecth, The Netherlands, 1986; p 27.
(3) (a) Shima, N. *J. Phys. Soc. Jpn.* **1982**, *51*, 11; **1983**, *52*, 578. (b) Bullett, D. W. *J. Phys. C: Solid State Phys.* **1982**, *15*, 3069. (c) Whangbo, M.-H.; Gressier, P. *Inorg. Chem.* **1984**, *23*, 1305.
(4) Bullett, D. W. *J. Phys. C: Solid State Phys.* **1979**, *12*, 277.
(5) Whangbo, M.-H.; Hoffmann, R. *J. Am. Chem. Soc.* **1978**, *100*, 6093.
(6) Hoffmann, R. *J. Chem. Phys.* **1963**, *39*, 1397. A modified Wolfsberg-Helmholz formula was used to calculate the off-diagonal H_{ij} values: Ammeter, J. H.; Bürgi, H.-B. Thibeault, J.; Hoffmann, R. *J. Am. Chem. Soc.* **1978**, *100*, 3686.

0020-1669/90/1329-1401$02.50/0